Cellular Senescence and Longevity of Osteophyte-Derived Mesenchymal Stem Cells Compared to Patient-Matched Bone Marrow Stromal Cells

Sanjleena Singh, Navdeep Dhaliwal, Ross Crawford, and Yin Xiao*

Institute of Health and Biomedical Innovation, Queensland University of Technology, Brisbane, QLD 4059, Australia

ABSTRACT

This study aimed to determine the cellular aging of osteophyte-derived mesenchymal cells (oMSCs) in comparison to patient-matched bone marrow stromal cells (bMSCs). Extensive expansion of the cell cultures was performed and early and late passage cells (passages 4 and 9, respectively) were used to study signs of cellular aging, telomere length, telomerase activity, and cell-cycle-related gene expression. Our results showed that cellular aging was more prominent in bMSCs than in oMSCs, and that oMSCs had longer telomere length in late passages compared with bMSCs, although there was no significant difference in telomere lengths in the early passages in either cell type. Telomerase activity was detectable only in early passage oMSCs and not in bMSCs. In osteophyte tissues telomerase-positive cells were found to be located perivascularly and were Stro-1 positive. Fifteen cell-cycle regulator genes were investigated and only three genes (*APC*, *CCND2*, and *BMP2*) were differentially expressed between bMSC and oMSC. Our results indicate that oMSCs retain a level of telomerase activity in vitro, which may account for the relatively greater longevity of these cells, compared with bMSCs, by preventing replicative senescence. J. Cell. Biochem. 108: 839–850, 2009.   © 2009 Wiley-Liss, Inc.

KEY WORDS: OSTEOPHYTE; MESENCHYMAL STEM CELL; TELOMERE LENGTH; TELOMERASE ACTIVITY; LONGEVITY; SENESCENCE; OSTEOARTHRITIS

Mesenchymal stem cells (MSCs) have a central role in regenerative medicine because of their multipotent nature and ability for self-renewal. Morphological and proteomic characteristics of MSCs, in particularly bone marrow stromal cells (bMSCs), have been extensively studied and are used for their identification. In our previously published study, MSCs were isolated and characterized from osteophyte tissues and it was shown that osteophyte-derived mesenchymal cells (oMSCs) were comparable to bMSCs with respect to morphology, cell surface antigen expression, differentiation potentials, and immunological response. The oMSCs were also found to have a much greater capacity for population doublings than bMSCs [Singh et al., 2008].

MSCs from various tissues have been isolated and compared to bMSCs, but there are no studies, to our knowledge, comparing site-specific differences between cells from the same patients. In fact, one of the major hurdles facing the successful therapeutic application of bMSCs is the limited number of MSCs that can be generated from bone marrow due to their limited lifespan in vitro. It is known that bMSCs only have in vivo telomerase activity and readily succumb to replicative senescence, limiting their in vitro proliferation potential [Banfi et al., 2002]. As far as we know, there are no published studies that compare telomere lengths of MSCs from different niches, the involvement of genes regulating cell cycle, and their effect on cell longevity or proliferative capacity with respect to bMSC.

The longevity of a cell population depends on the phenomenon of replicative senescence, first described by Hayflick [1985]. Replicative senescence is marked by the progressive shortening of the telomeres and various other mechanisms such as changes in gene expression during long-term culture condition resulting in DNA damage. These factors play a role in promoting cellular aging, characterized by MSCs becoming enlarged and irregular in shape and ultimately a complete cessation of proliferation. Telomerase reverse transcriptase (hTERT) is a highly specialized ribonucleoprotein complex, which maintains telomere length by adding telomeric TTAGGG repeats to the 3′ ends of human chromosomes [Broccoli et al., 1995]. This process protects the 3′ end of the single-strand DNA overhang which has been shown to be most important for cellular integrity [Blackburn, 2001; Baird, 2008]. In the event that telomerase activity is inhibited or suppressed, telomeres become shortened and cells rapidly succumb to senescence and apoptosis. Telomerase activity has been found to be widely distributed among renewing human tissues and concentrated in the areas of stem cells

and actively multiplying transit cells [Rubin, 2002]. Evidence of telomerase activity in normal somatic tissues have been found in bone marrow and peripheral blood leukocytes [Broccoli et al., 1995; Counter et al., 1995; Hiyama et al., 1995], epidermis [Harle-Bachor and Boukamp, 1996] as well as in cells that have "replenishing" roles such as cells in the skin and gut mucosa. Dysregulation of telomerase activity results in uncontrolled malignant tumor growth [Dhaene et al., 2000]. Several studies have shown that cancer cells also have increased telomerase activity which stops telomere shortening and enhances their self-renewal ability and resistance to apoptosis, effectively rendering them immortal [Fujiwara, 2009; Proctor et al., 2009; Schmelzer and Reid, 2009; Shaker et al., 2009].

The loss of telomerase activity has been associated with disease and it has been demonstrated in vitro in diseased osteoblasts and chondrocytes. This may be of significance to the progression of osteoarthritis (OA) and may also be correlated with osteopenia [Yudoh and Nishioka, 2004]. However, telomerase activity in osteophyte tissues and cells is still not known.

The aim of this study was to compare the longevity of patient-matched bMSCs and oMSCs and to determine what relationship exists between telomerase activity, telomere length, and cell senescence with respect to a cell type's in vitro longevity.

MATERIALS AND METHODS

TISSUE SAMPLES

Osteophyte tissues were collected from five patients after informed consent was given. The patients were between 65 and 78 years of age undergoing elective knee replacement surgery. Bone marrow was also collected from the same patients by bone marrow aspirate [Singh et al., 2008]. All procedures were done in accordance with the ethics guidelines of the Queensland University of Technology and Prince Charles Hospital, Brisbane, Australia.

MSC CULTURE AND CHARACTERIZATION

The osteophyte tissues were placed in sterile containers with 10 ml of Hanks buffer (Gibco, Invitrogen, Mount Waverley, VIC, Australia). Superficial fibrous cartilage was discarded, and 2 mm segments were dissected along the tissue and placed in six-well plates with 2 ml of low glucose DMEM (Gibco) with 10% (v/v) fetal bovine serum (FBS) (HyClone, Logan, UT) and 1% (v/v) penicillin and streptomycin (Gibco). Confluent cultures were trypsinized and passaged before cryopreservation. bMSCs and oMSCs were isolated and characterized according to a previously published method [Mareddy et al., 2007; Singh et al., 2008]. Briefly, bMSCs were isolated by Lymphoprep (Axis-Sheild PoC AS, Oslo, Norway) gradient sedimentation and oMSCs were isolated from explant cultures.

Cells isolated from osteophyte tissue and bone marrow aspirates at passage 4 were trypsinized and incubated for 30 min on ice with antibodies for the following cell surface antigens: CD45 (leukocyte marker), CD34 (hematopoietic stem cells), CD44, CD29, CD166 (adhesion related), CD90, CD105, CD73 (mesenchymal/stromal stem cells), MHC I, and MHC II. All antibodies were from Becton Dickinson Biosciences (NJ). Single-color staining was performed using a phycoerythrin (PE)-conjugated secondary antibody (Becton Dickinson Biosciences, NJ) and analyzed using a fluorescence-activated cell sorter (FACS Vantage SE; Becton Dickinson, UK) using a 575-nm band pass filter for red PE fluorescence. Data were analyzed using WinMDI 2.8 software.

Cells at passages 3–5 were differentiated into chondrocytes according to micro-mass pellet culture. Briefly, cells (2.5×10^5) were placed in serum-free medium consisting of high glucose DMEM supplemented with 10 ng/ml TGF-β_3, 100 nM dexamethasone, 50 μg/ml ascorbic acid 2-phosphate, 100 μg/ml sodium pyruvate, 40 μg/ml proline, and a commercial preparation of ITS-plus (final concentration: 6.25 μg/ml insulin, 6.25 μg/ml transferrin, 6.25 μg/ml selenous acid, 5.33 μg/ml linoleic acid, and 1.25 mg/ml bovine serum albumin) (Sigma–Aldrich, NSW, Australia). Cell pellets were formed by centrifugation at 500g for 15 min, and then cell pellets were cultured in the chondrogenetic induction medium mentioned above for a further 3 weeks. The pellets were fixed with 4% paraformaldehyde and matrix deposition of proteoglycans was detected by Alcian blue stain. Osteogenic differentiation of subconfluent osteophyte monolayers (passages 3–5) was induced by medium containing 50 μM ascorbic acid 2-phosphate, 10 mM β-glycerol phosphate, and 100 nM dexamethasone in DMEM with 10% FBS. This medium was changed twice weekly for up to 3 weeks. Following 4% paraformaldehyde fixation, cell and matrix mineralization was detected by Alizarin red stain for calcium deposits. Confluent cultures of oMSCs and bMSCs at 3–5 passages undergoing adipogenic differentiation were induced using medium containing 0.5 mM isobutylmethyl xanthine, 100–200 μM indomethacin, 1 μM dexamethasone, and 10 μg/ml insulin in DMEM with 10% FBS. The cells were treated in this medium for 3 days, and then the medium was changed to adipogenic maintenance medium (DMEM with 10% FBS and 10 μg/ml insulin) alone for 24 h. After three cycles, cells were cultured in maintenance media for another 21 days. Cells were fixed with 4% paraformaldehyde and stained with oil red 0 to detect the lipid droplets in the differentiated cells.

CELL SENESCENCE ASSAY

Cytochemical staining for senescence associated β-galactosidase assay was performed using a β-galactosidase staining kit (Cell Signaling Technology, Beverly, MA). Cells from passage 4 (P4) and passage 9 (P9) were seeded at a density of 2×10^4/well into four-well plates and allowed to attach overnight, then washed with PBS, fixed, and incubated overnight at 37°C with X-gal chromogenic substrate at pH 6.0 according to manufacturer's protocol. The color development was observed under light microscope and the image was captured at 100× magnification. The percentage of stained cells was calculated from the averages from five MSC cultures from both early and late passages.

CELL PROLIFERATION (^{3}H LEUCINE INCORPORATION)

To compare the capacity of cell proliferation between oMSCs and bMSCs, cell proliferation was conducted at the 4th and 9th passage using ^{3}H leucine incorporation assay [Singh et al., 2008]. Briefly, BMSCs and oMSCs at the 4th and 9th passage were seeded in 24-well plates at 1×10^4 cells per well. ^{3}H-leucine was added at (1 μCi/ml) to each well. Proliferation was assessed on day 2. Cell number was quantified by the amount of ^{3}H leucine-labeled protein. Briefly, cells were washed with Hank buffer salt solution twice, then incubated

with 2 ml of 10% trichloroacetic acid. This was followed by two washes with distilled water and then incubated with 1 ml of caustic triton overnight. To produce a homogenous protein solution, plates were placed on a plate shaker for 1 h, then 100 µl samples were aliquoted into 96-well isotope plate. Radioactivity was measured by a scintillation counter (Wallac Microbeta Trilux, USA). All experiments were performed in triplicate.

TELOMERE LENGTH ASSAY

This protocol was adapted from Cawthorn et al. [Cawthon, 2002]. Telomere (T) PCR and single copy gene (S) PCR were performed in separate plates. Two master mixes of PCR reagents—one with the T primer pair and one with the S primer pair—were prepared. Thirty microliters of T master mix was added to each sample well and standard curve well of the first plate, and 30 µl of S master mix was added to each sample well and standard curve well of the second plate. For each individual whose T/S ratio was assayed, three identical 20 µl aliquots of the DNA sample (35 ng/aliquot) were added to Plate 1 and another three aliquots were added to the same well positions in Plate 2. For each standard curve, one reference DNA sample was serial diluted in TE-4 by ~1.68-fold per dilution to produce five concentrations of DNA ranging from 0.63 to 5 ng/µl, and which were then distributed in 20 µl aliquots to the standard curve wells of each plate.

The final concentrations of reagents in the PCR were 150 nM 6-ROX and $0.2\times$ Sybr Green I (Molecular Probes), 15 mM Tris–HCl, pH 8.0, 50 mM KCl, 2 mM $MgCl_2$, 0.2 mM each dNTP, 5 mM DTT, 1% DMSO, and 1.25 U AmpliTaq Gold DNA polymerase (Applied Biosystems, Scoresby, VIC, Australia). The final telomere primer concentrations were: T1, 270 nM; T2, 900 nM. The final 36B4 (single copy gene) primer concentrations were: 36B4u, 300 nM; 36B4d, 500 nM. The primer sequences were:

T1: 5′-GGTTTTTGAGGGTGAGGGTGAGGGTGAGGGTGAGGGT-3′.
T2: 5′-TCCCGACTATCCCTATCCCTATCCCTATCCCTATCCCTA-3′.
36B4u: 5′-CAGCAAGTGGGAAGGTGTAATCC-3′.
36B4d: 5′-CCCATTCTATCATCAACGGGTACAA-3′.

All polymerase chain reactions were performed using the ABI Prism 7700 Sequence Detection System (Applied Biosystems). The thermal cycling profiles were as follows: 10 min activation step at 95°C; then for the telomere Plate 18 cycles of 95°C for 15 s, 54°C for 2 min and for the 36B4 Plate 30 cycles of 95°C for 15 s, 58°C for 1 min. The data were analyzed using the SDS 1.7 software to generate a standard curve for each plate and to determine the dilution factors of standards corresponding to the T and S amounts in each sample.

TELOMERASE ACTIVITY ASSAY

Telomerase activity in P4 and P9 oMSC and bMSC was assayed using a TRAPeze Detection Kit (Chemicon International, CA). Briefly, cells were lysed and endogenous telomerase activity evaluated in the supernatant based on its extension of a telomerase template. Products were visualized on 2% acrylamide gels stained in SYBRGreen (Invitrogen) and analyzed by Fluorimager SI (Molecular Dynamics, CA). The presence of telomerase activity was indicated by a ladder of 6-mer products as shown by the positive control.

FLOW CYTOMETRIC ANALYSIS

Passage 4 and 9 oMSCs and bMSCs were analyzed for the presence of telomerase by flow cytometry. Cells (3×10^4) were used for the assay by fixation into a well of 96-well plate containing 100 µl of 4% paraformaldehyde solution for 15 min, washed twice with washing buffer (PBS with 0.01% BSA) by centrifuging the cells at a speed of 1,350 rpm for 3 min each, then permeabilized with 95% ice-cold methanol for 30 min, followed by a further two washes. The cells were incubated with the hTERT rabbit polyclonal antibody EST21A (Alpha Diagnostic International, TX; 1:50 dilution) at 4°C overnight. On day 2 the cells were washed twice with washing buffer and incubated with a PE-conjugated secondary antibody (Becton Dickinson Biosciences, NJ) for 30 min at room temperature.

For Stro-1 expression, cells were incubated with a Stro-1 antibody (Becton Dickinson Biosciences, NJ) for 30 min, washed twice with PBS, and incubated with Alexa Fluor 488-conjugated secondary antibody (Becton Dickinson Biosciences, NJ) for 20 min, then washed and diluted in 50 µl of staining buffer before analysis. The fluorescence intensity of positively stained samples was compared to unstained, as well as isotope-matched negative controls. Mononuclear cells were gated according to a combination of forward scatter (FCS), side scatter (SSC), and absence of PE fluorescence.

QUANTITATIVE REAL–TIME PCR

oMSCs and bMSCs at P4 were analyzed for the mRNA expression of 15 cell-cycle-related genes (Table I). Total RNA was extracted with Trizol (Invitrogen) according to the manufacturer's instructions. Both primers and reagents were supplied as part of the Superarray RT^2 Profiler plates (Superarray Bioscience Corporation, Jomar Biosciences, Kensington, SA, Australia) for human stem-cell-related genes. PCR cycle conditions were as follows: 95°C for 5 min followed by 40 cycles at 95°C for 30 s and 58°C for 30 s. Cycle threshold (C_t) values were used to perform calculations. The relative expressions of genes were calculated on the data analysis template provided in the kit (C_t values were normalized against five housekeeping genes). The expression of mRNA of each gene relative to housekeeping mRNA is expressed as $2^{-\Delta C_t}$. The P-value and fold changes were calculated by the functions in the template.

KARYOTYPING

Passage 4 and 9 oMSCs and bMSCs were sent to Sullivan and Nicolaides Pathology Services (Brisbane, QLD, Australia) for karyotyping study. The cells were processed and metaphases of cells were Q-banded and chromosomes karyotyped according to the recommendations set out in the International System for Human Cytogenetic Nomenclature.

IMMUNOHISTOCHEMISTRY

Osteophyte tissues from five patients were demineralized, processed, and embedded in paraffin wax. The tissues were cut in 5 µm serial sections for immunohistochemical staining. Briefly, sections were incubated with a 1:100 dilution of the hTERT antibody EST21A or 1:100 dilution of Stro-1 antibody overnight at 4°C. The sections were incubated with a biotinylated swine-antimouse, rabbit, goat

TABLE I. Cell-Cycle Regulator Gene Expression in oMSCs and bMSCs

RefSeq	Symbol	Description	Gene name	oMSC/bMSC	*P*-value
NM_001237	CCNA2	Cyclin A2	CCN1/CCNA	1.96	0.3054
NM_053056	CCND1	Cyclin D1	BCL1/D11S287E	−1.15	0.6379
NM_001759	CCND2	Cyclin D2	KIAK0002	−2.93	0.0459
NM_001238	CCNE1	Cyclin E1	CCNE	−1.48	0.1380
NM_001786	CDC2	Cell division cycle 2, G1 to S and G2 to M	CDC28A/CDK1	1.68	0.3849
NM_001791	CDC42	Cell division cycle 42 (GTP binding protein, 25 kDa)	CDC42Hs/G25K	−1.24	0.6716
NM_016204	GDF2	Growth differentiation factor 2	BMP-9/BMP9	1.32	0.2594
NM_020634	GDF3	Growth differentiation factor 3	GDF3	−4.49	0.8135
NM_001527	HDAC2	Histone deacetylase 2	RPD3/YAF1	−1.42	0.8208
NM_032188	MYST1	MYST histone acetyltransferase 1	MOF/hMOF	1.39	0.7213
NM_007067	MYST2	MYST histone acetyltransferase 2	HBO1/HBOA	1.02	0.8178
NM_016948	PARD6A	Par-6 partitioning defective 6	PAR-6A/PAR6	−1.03	0.8167
NM_000321	RB1	Retinoblastoma 1 (including osteosarcoma)	OSRC/RB	−1.90	0.7854
NM_001200	BMP2	Bone morphogenic protein 2	BMP2A	3.37	0.0195
NM_000038	APC	Adenomatous polyposis coli	DP2/DP3	−1.47	0.0347

antibody (Dako Multilink, CA) for 15 min, followed by 15 min incubation with horseradish peroxidase-conjugated avidin–biotin complex. Antibody complexes were visualized by the addition of a buffered diaminobenzidine (DAB) substrate for 4 min and lightly counterstained with Mayer's hematoxylin.

RESULTS

MESENCHYMAL STEM CELLS IN OSTEOPHYTE TISSUE AND OSTEOPHYTE-DERIVED CELLS (oMSCS)

Cells in osteophyte tissue showed expression for the primitive mesenchymal marker Stro-1, especially in areas with new tissue formation (Fig. 1C,D). Immunohistochemical analysis found a large number of cells around the newly formed bone tissue staining positive for Stro-1 (Fig. 1D). The presence of telomerase-positive cells was also identified in the osteophyte tissue (Fig. 1E,F). Most telomerase-positive cells were spatially located in perivascular sites (Fig. 1E) and new bone-forming areas adjacent to the newly formed osteoids (Fig. 1F). No Stro-1 and telomerase-positive cells were found in mature tissue in osteophyte indicating that telomerase-positive cells involved in renewing human tissues and concentrated in the areas of stem cells and actively multiplying transit cells.

Stro-1 expression in oMSCs and bMSCs was also studied by flow cytometry analysis (Fig. 2) and showed that the percentage of Stro-1-positive cells was greater in oMSCs than in bMSCs both in early (P4) and late (P9) passage cultures. This indicated that oMSCs retained the surface antigen expression of Stro-1 even after extensive population doublings, whereas bMSCs at P9 showed a significant decrease of Stro-1-positive cells compared to oMSC ($P < 0.02$).

CHARACTERIZATION OF OSTEOPHYTE-DERIVED MSCs (oMSCs)

MSCs were successfully cultured from osteophyte tissues collected from patients undergoing knee replacement surgery. These cells appeared as typical MSCs, adhering to culture plastic and having a fibroblastic morphology within 24 h (Fig. 3A,i). These cells were able to differentiate into the mesenchymal lineages producing osteogenic (Fig. 3A,ii), chondrogenic (Fig. 3A,iii), and adipogenic (Fig. 3A,iv) cultures. oMSC cultures were expanded greater then 10 passages and

were able to be re-cultured from frozen stocks that had been stored in liquid nitrogen (results not shown).

The surface antigen phenotype of oMSCs was similar to that of a normal MSCs (Fig. 3B). They did not express major histocompatability complex class II (MHC II), but did express the class I (MHC I) isoform. There was no contamination of oMSC cultures with leukocytes (CD45) and hematopoietic stem cells (CD34). As there is no specific surface antigen marker for MSCs, a panel of MSC "indicative markers" were used, including antigens involved in cell adhesion (CD166, CD44, CD29) and putative stem cell markers (CD90, CD105, CD73). oMSCs and bMSCs expressed a similar MSC-like profile of these markers (results of bMSCs not shown).

β-GALACTOSIDASE EXPRESSION IN oMSCs AND bMSCs

β-Galactosidase staining in both oMSCs and bMSCs cultures increased with the number of passages (Fig. 4A). Interestingly, bMSCs showed significantly higher cell numbers with the expression of β-galactosidase compared to oMSCs in P9. The number of β-galactosidase-positive cells in early passage was low at 0–4% in oMSCs and 8–11% in bMSCs at P4 culture; however, at P9, β-galactosidase-positive cells increased to 20–24% in oMSCs and 86–92% in bMSCs (Fig. 4B). The percentage of β-galactosidase-positive cells in bMSCs was significantly higher than that in oMSCs ($P < 0.002$, n = 5). In bMSCs increase of β-galactosidase-positive cells in the late passage was correlated with the decrease of cell proliferation. There was a significant decrease in cell proliferation in P9 bMSCs compared with P4 bMSCs and P9 oMSCs. In oMSCs there was a trend of decrease in cell proliferation during passages; however, no statistically significant difference in cell proliferation was found between P9 and P4 oMSCs (Fig. 4C).

TELOMERE LENGTH AND TELOMERASE ACTIVITY IN oMSC AND bMSC

There was a significant decline of telomere length detected in matched P9 oMSCs and bMSCs compared to the corresponding P4 cells (Fig. 5). No significant difference was seen between oMSCs and bMSCs at P4; however, at P9 oMSC telomere length was significantly higher than bMSC telomere length ($P < 0.01$).

Compared with the positive control, telomerase activity was significantly decreased in both P4 and P9 oMSCs and bMSCs. In P4
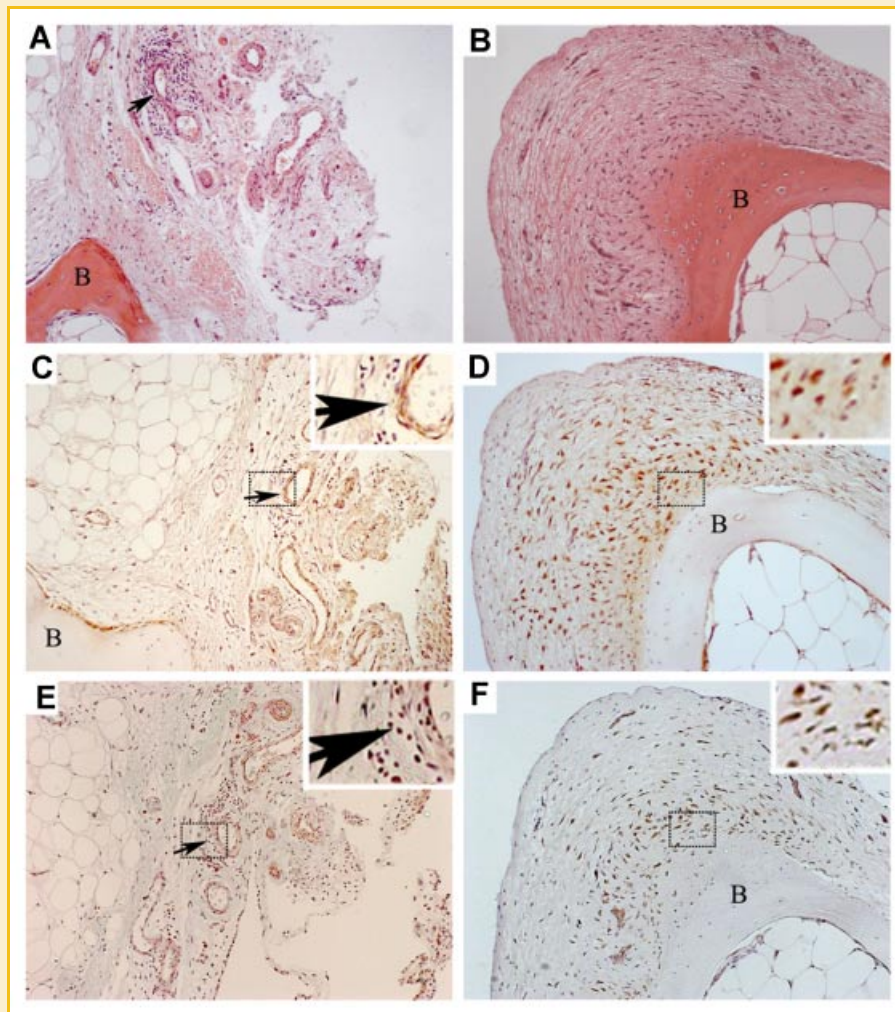
Fig. 1. Stro-1 and telomerase expression in osteophyte tissues. A vessel concentrated area (A) and a new bone formation area (B) were selected from osteophyte tissues. Cells in osteophyte tissue showed expression for the primitive mesenchymal marker Stro-1 in cells related to vessels (C) and new tissue formation (D). The presence of telomerase-positive cells was also identified in the osteophyte tissue (E,F). Most telomerase-positive cells were spatially located in perivascular sites (E) and new bone-forming areas adjacent to the newly formed osteoids (F). A targeted area selected in C–F was enlarged and showed in the upright corner to give a better view of the positive staining. (Image magnification: 200×; B = bone; arrow = blood vessel.) [Color figure can be viewed in the online issue, which is available at www.interscience.wiley.com.]

oMSCs low-level telomerase activity was detectable, showing a non-continuing low molecular banding compared to controls, whereas no activity was detectable in either P4 or P9 bMSCs or in P9 oMSCs (Fig. 6A). Flow cytometry analysis of hTERT also revealed that the percentage of telomerase-positive cells was significantly greater in P4 oMSCs compared to P4 and P9 bMSCs and P9 oMSCs ($P < 0.01$; Fig. 6B,C). However, in both bMSCs and oMSCs there was a precipitous loss of telomerase activity after extensive population doublings.

CYTOGENETIC KARYOTYPE ANALYSIS OF oMSCs AND bMSCs

Karyotypic analysis of P4 and P9 bMSCs (Fig. 7A) and oMSCs (Fig. 7B) did not reveal any aneuploidy, abnormal metaphases, and extensive translocation of the chromosomes or changes in the copy number as is observed in some cancer or tumor cells. Furthermore, when compared to bone marrow cells the cytogenetic analysis revealed a normal chromosomal number and Q-banding pattern

indicating that chromosome mitosis was typical for both cell types (Fig. 7).

CELL-CYCLE REGULATOR GENE EXPRESSION IN oMSCs AND bMSCs

Fifteen genes involved in cell-cycle regulation, modulation of chromatin, and telomerase were analyzed in P4 oMSCs and bMSCs by real-time PCR. The results showed that 12 out of the 15 cell-cycle regulatory genes were expressed equally in both oMSCs and bMSCs ($P > 0.05$, Table I), but that there was a significantly differential expression of three genes in matched oMSCs and bMSCs samples ($P < 0.05$, Table I). Cyclin D2 (CCND2) and adenomatous polyposis coli (APC), both directly related to cell-cycle regulation, were down-regulated in oMSC compared to bMSCs; interestingly, bone morphogenetic protein 2 (BMP2) was more than threefold up-regulated in oMSC.
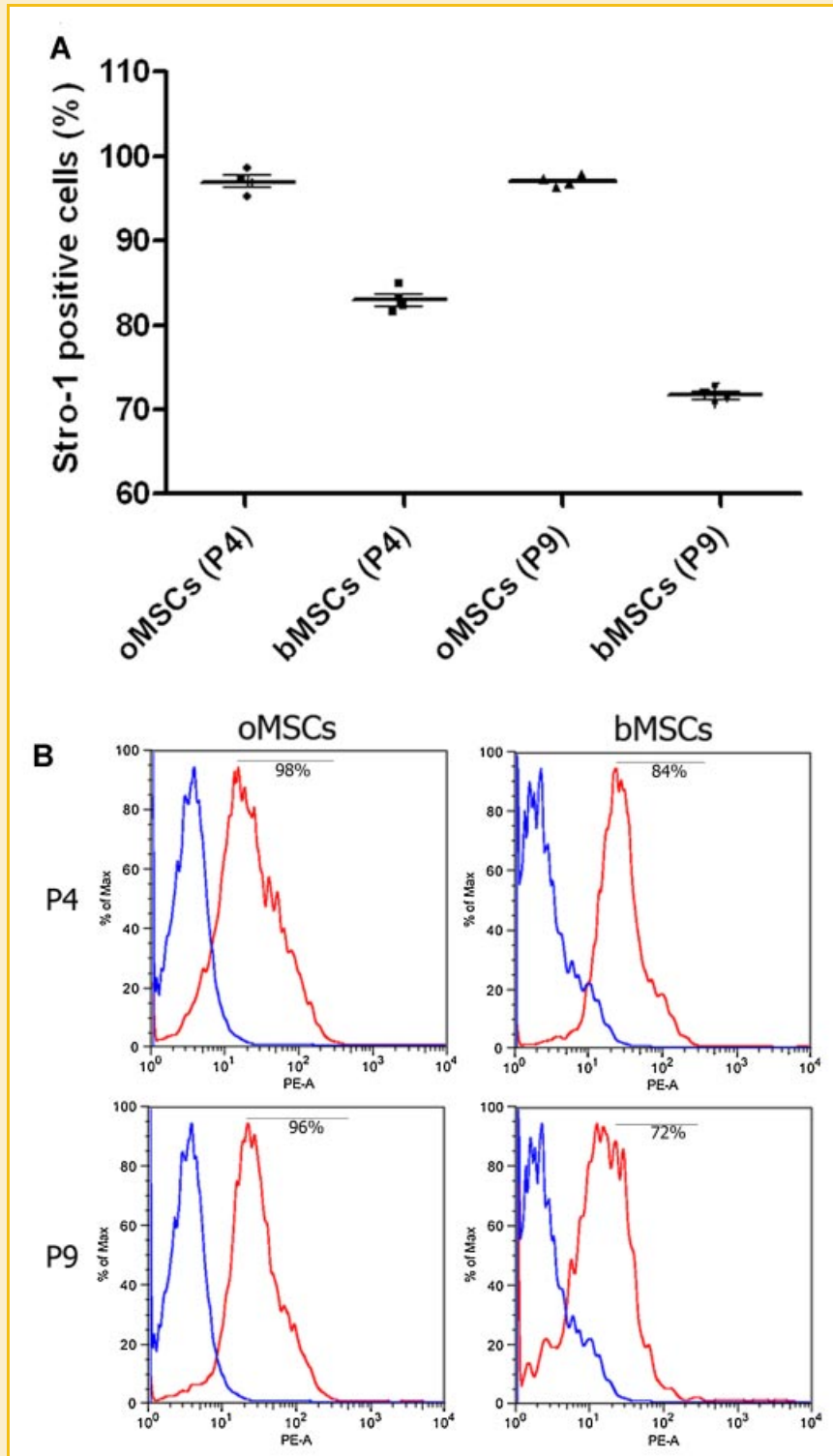
Fig. 2. Flow cytometry study (FACS) of Stro-1 expression in oMSCs and bMSCs. The percentage of Stro-1–positive cells was greater in oMSCs than in bMSCs both in early (P4) and late (P9) passage cultures (A). (B) A representative histogram plot of the Stro-1 FACS results from oMSCs and bMSCs (blue peak: negative control; red peak: positive expression). [Color figure can be viewed in the online issue, which is available at www.interscience.wiley.com.]
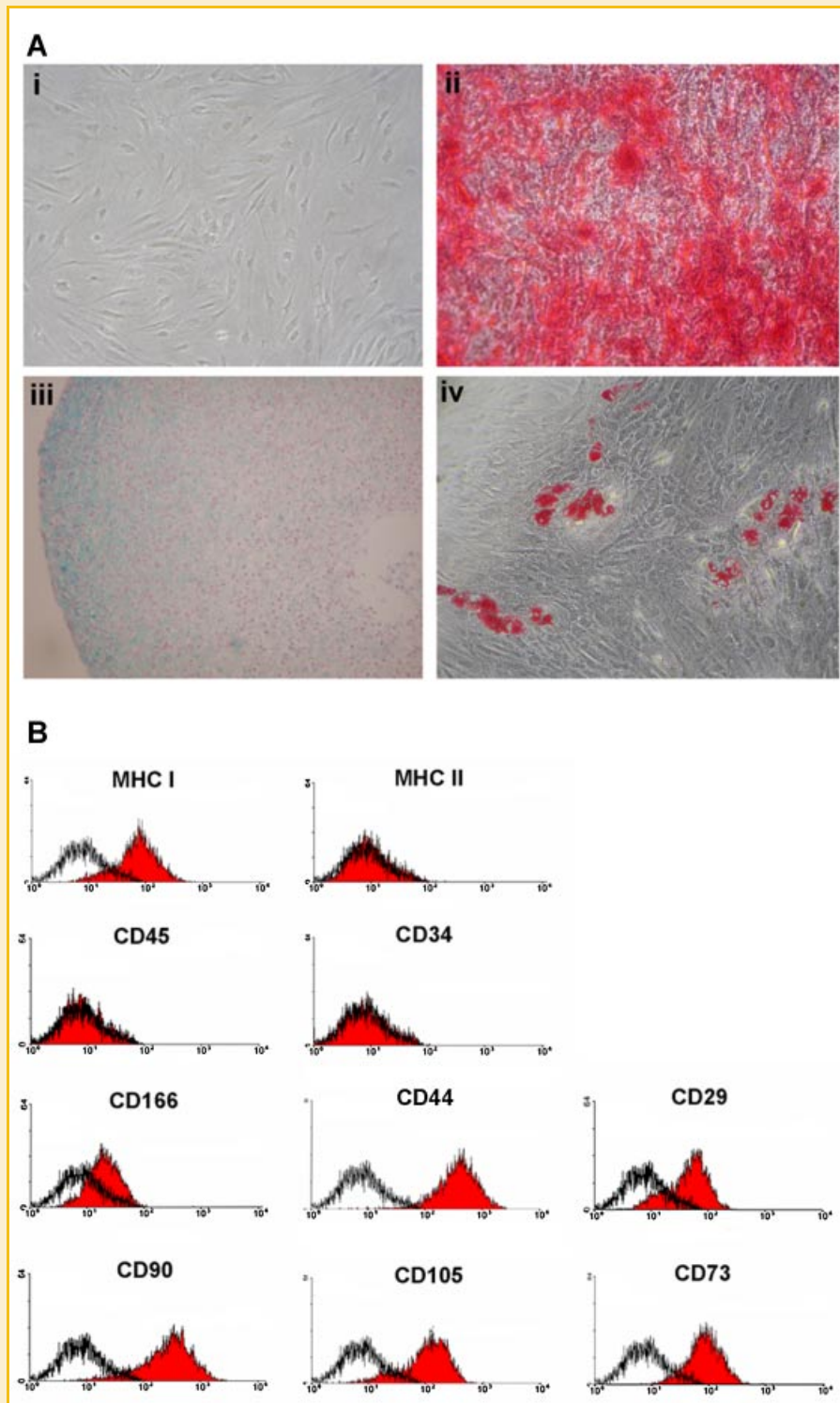
Fig. 3. Characterization of oMSCs. (A,i) Passage 4 oMSCs exhibiting a typical attached MSC fibroblastic morphology. (ii) Osteogenic differentiation—calcium deposition stained by Alzarin red. (iii) Chondrogenic differentiation—proteoglycan deposition stained by Alician blue in pellet culture. (iv) Adipogenic differentiation—lipid droplets stained with Oil Red O (all image magnification $= 100\times$). (B) Immunophenotypic characterization of oMSCs showed that oMSCs expressed a typical MSC surface antigen profile, lacking MHC II expression, absence of contamination with leukocytes (CD45) and hematopoietic stem cells (CD34), and expressing various adhesion (CD166, CD44, CD29) and stem cell–like (CD90, CD105, CD73) molecules. Graphs are representatives of five oMSC cultures. [Color figure can be viewed in the online issue, which is available at www.interscience.wiley.com.]
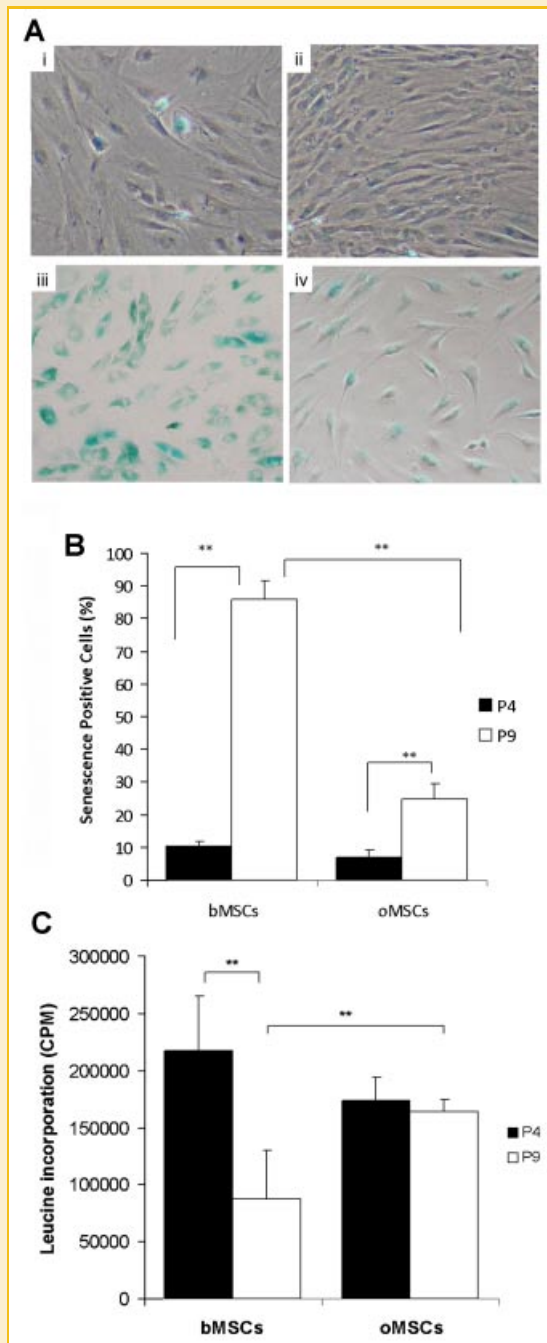
Fig. 4. β‐Galactosidase expression in oMSCs and bMSCs. β‐Galactosidase staining in P4 (i) and P9 (iii) bMSCs and P4 (ii) and P9 (iv) oMSCs showed an increase of positive cells with the number of passages (A). bMSCs (iii) showed significantly higher cell numbers with the expression of β‐galactosidase compared to oMSCs (iv) in P9. The number of β‐galactosidase positive cells in early passage was low showing 0–4% in oMSCs and 8–11% in bMSCs at P4 culture (B). At P9, positive cells increased to 20–24% in oMSCs and 86–92% in bMSCs (B). The percentage of cells positively to β‐galactosidase staining in bMSCs was significantly higher than in oMSCs ($P < 0.002$, n = 5). Significantly decreased cell proliferation was noted in P9 bMSCs when compared with P4 bMSCs and P9 oMSCs (C). In oMSCs, there was a trend of decrease in cell proliferation during passages; however, no statistically significant difference in cell proliferation was found between P9 and P4 oMSCs (C). [Color figure can be viewed in the online issue, which is available at www.interscience.wiley.com.]
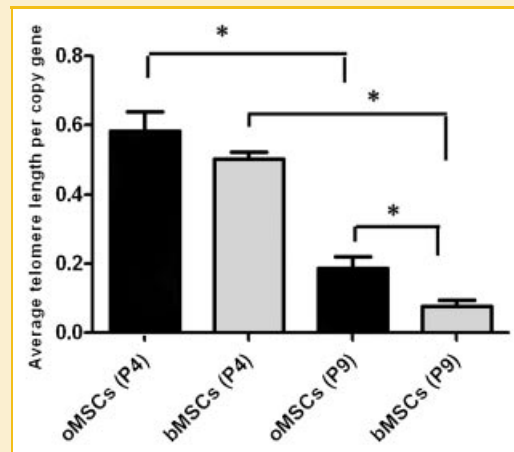
Fig. 5. Telomere length in oMSCs and bMSCs. There was a significant decline of telomere length detected in matched P9 oMSCs and bMSCs compared to the corresponding P4 cells. No significant difference was seen between oMSCs and bMSCs at P4; however, at P9 oMSC telomere length was significantly higher than bMSC telomere length ($P < 0.01$).

DISCUSSION

OA is a frequent cause of chronic disability and is highly prevalent in persons over the age of 65. The etiology of OA is poorly understood and current treatments merely alleviate the symptoms. As yet there is no way of reversing or significantly delaying the disease progression. Osteophytes form at the margins of articular cartilage in the osteoarthritic joint and their formation is associated with mesenchymal precursors from the chondro‐synovial junction, probably in response to altered biomechanics and remodeling of the underlying bone [van der Kraan and van den Berg, 2007]. We recently characterized osteophyte‐derived cells as MSCs and found that these cells were capable of retaining proliferative capacities at higher passage numbers compared with patient‐matched bMSCs. It is not clear that the relationship between tissue‐derived MSCs and bMSCs even though bone marrow has been considered to be the major reservoir of MSCs. Microenvironment where MSCs residence plays an imperative role in determining stem cell fate. In the current study, we found that the proliferative potential of MSCs from bone marrow and osteophytes appeared to be closely linked to telomere length, which is controlled by telomerase activity, and Stro‐1 expression. However, there was no statistically significance in oMSC proliferation between P9 and P4, even though telomere length and telomerase activity were significantly decreased in P9 oMSCs. The significantly higher telomerase activity in the early passage oMSCs (P4) and the retaining of primitive marker Stro‐1 in the late passage oMSCs (P9) may be responsible for the maintenance of proliferation in P9 oMSCs. Previous studies have showed that stem cells in their niches have longer telomeres in comparison to their more differentiated counterparts [Flores et al., 2008], but none of the studies have compared site‐specific differences in MSCs from the same patient. This study sought to address this knowledge gap by characterizing the presence of the telomerase subunit as well as telomerase activity and cellular senescence in oMSCs compared to
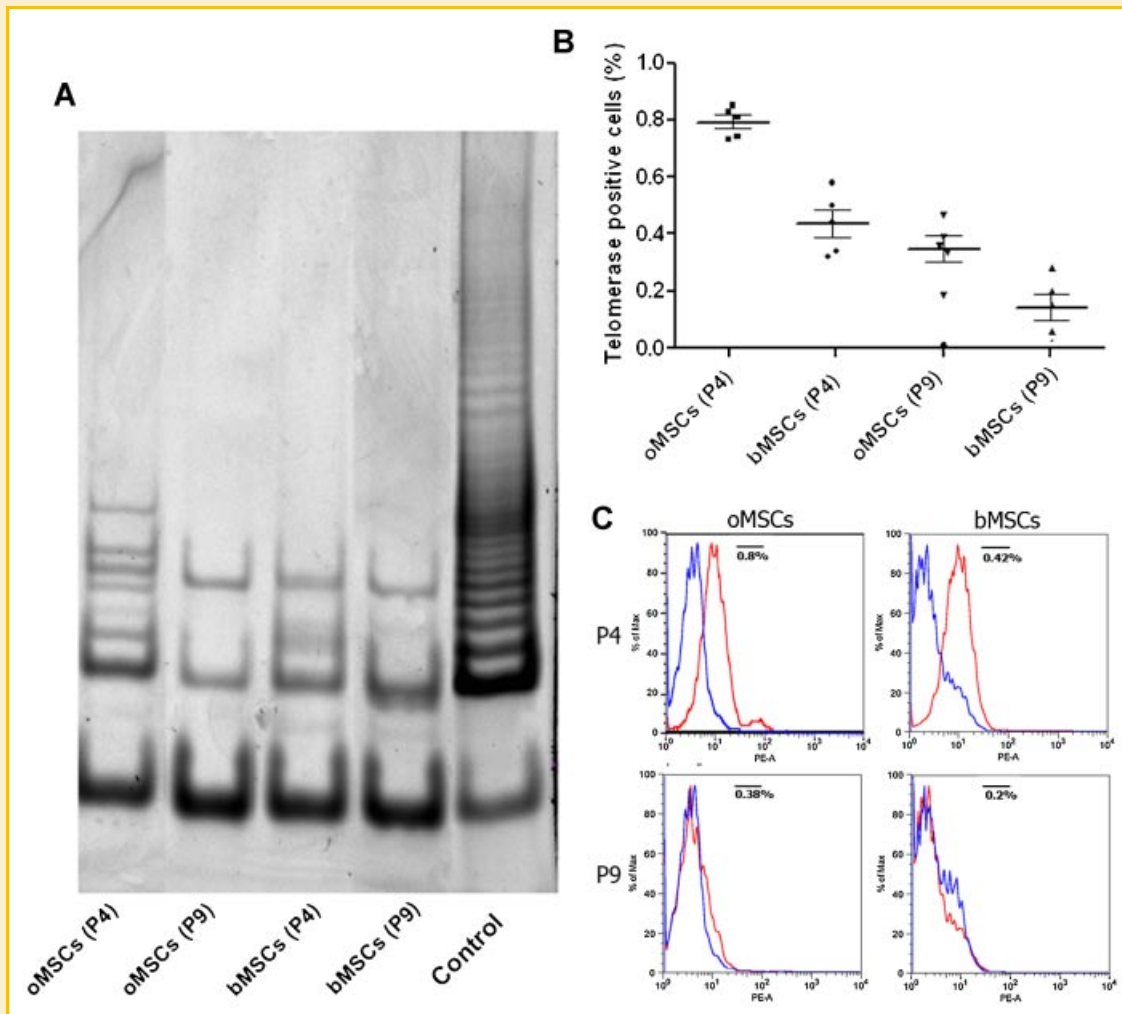
Fig. 6.   Telomerase activity in bMSC and oMSCs. Compared with the positive control, telomerase activity was significantly decreased in both P4 and P9 oMSCs and bMSCs (A). In P4 oMSC low-level telomerase activity was detectable, showing a non-continuing low molecular banding compared to controls, but no activity was detectable in either P4 or P9 bMSCs or in P9 oMSCs (A). Flow cytometry analysis of hTERT also revealed that the percentage of telomerase-positive cells was significantly greater in P4 cultures of oMSCs compared to P4 bMSCs and P9 cultures of bMSCs and oMSCs ($P < 0.01$; B). (C) A representative histogram plot of the hTERT FACS results from oMSCs and bMSCs (blue peak: negative control; red peak: positive expression). [Color figure can be viewed in the online issue, which is available at www.interscience.wiley.com.]

patient-matched bMSCs. Our data indicate that oMSC is not an immortalized cell, since they can enter cell senescence, has decreasing telomere length and normal karyotype, all in keeping with the current knowledge of MSC cultures. We also found that oMSCs may have some telomerase activity in the culture of early passages and are able to retain a primitive undifferentiated state.

Cell differentiation plays a crucial role in declining proliferative capacity. Stro-1 has been identified as a marker of primitive stem cells and does not present in committed progenitors [Simmons and Torok-Storb, 1991]. Our results show that >95% of oMSCs retained their primitive Stro-1-positive stem cell phenotype, whereas a significant decrease was seen in bMSCs. Previous studies have demonstrated that MSCs can be isolated from various regenerative tissues and that such MSCs have different functional properties including different long-term growth kinetics [Banfi et al., 2000; Kern et al., 2006]. Osteophyte tissues showed the presence of highly proliferating areas, having MSCs expressing the

Stro-1 marker. These results suggest that the presence of Stro-1-positive oMSCs may be carried over from the tissues and that human bone marrow cell populations contain partially differentiated progenitor cells, which may be the reason that there are relatively less Stro-1-positive bMSCs compared with oMSCs [Zimmermann et al., 2003].

Prior studies show that the enzyme, lysosomal, β-galactosidase (SA-β-gal) is active in senescent human fibroblasts, but not in quiescent, pre-senescent or pre-differentiated cells. There is an age-dependent increase in β-galactosidase expression as normal somatic cells invariably enter a state of irreversibly arrested growth and altered function after a finite number of cell divisions [Dimri et al., 1995]. oMSCs showed the same characteristics as bMSCs in that cells from both sources were prone to cellular aging in long-term culture; however, the percentage of senescent oMSC in early and late passages were less than bMSCs at the same population doublings. It has also been reported that the rate of senescence is
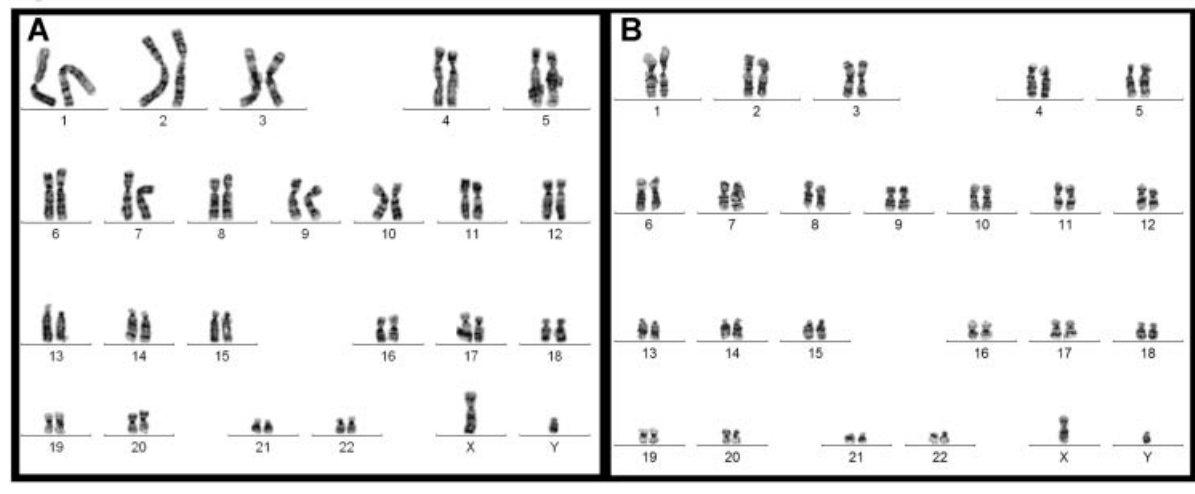
Fig. 7. Cytogenetic karyotype analysis of oMSCs and bMSCs. Representative pictures of karyotype analysis of P9 bMSCs (A) and P9 oMSCs (B) did not reveal any aneuploidy, abnormal metaphases, and extensive translocation of the chromosomes.

affected by the culture conditions and repeated passage at various densities [Colter et al., 2000; Fehrer et al., 2007]. In this study the culture conditions and seeding densities were therefore kept as similar as possible in both cell cultures.

The concept of "age-dependent" expression in cell cultures was very distinct, not only between passages, but also between cell sources [Fehrer et al., 2007]. When compared to our previously reported results for cell proliferation [Singh et al., 2008], oMSCs appeared to have either more primitive cells or be somehow more resistant to aging. Various studies have indicated that cellular aging may be, in part, due to critical size telomere length that leads to replicative senescence [Yang, 2008; Britt-Compton et al., 2009; Hanna et al., 2009; Wu et al., 2009]. Evidence suggests that stem cells maintain longer telomeres relative to other cells within the tissue, such as in lingual mucosa, where in situ hybridization has revealed longer telomeres in the basal cells [Aida et al., 2008] and stem cell compartments of the skin, small intestine, cornea, testis, and brain [Flores et al., 2008]. One study revealed that the mean terminal restriction fragment (TRF) may vary by as much as 5% in individuals [Parsch et al., 2004]. In the present study a simpler quantitative PCR-based assay was used to determine average telomere length. Our results indicate that at both early and late passages average telomere lengths were longer in oMSCs than bMSCs, which implies that oMSCs are capable of undergoing more population doublings than bMSC before reaching the critical point of growth arrest.

Given the immune privilege and replicative potential of MSC, the question has been raised whether MCSs may be more prone to undergo malignant transformation. Even though MSCs derived from healthy tissues do not appear to exhibit tumorigenic characteristics [Bernardo et al., 2007; Serakinci et al., 2008], it remains unclear whether MSCs derived from diseased tissues, such as osteophytes, show adverse cytogenetic variation in comparison to MSCs from bone marrow. It has been demonstrated clinically that most malignant cells will exhibit some type of chromosomal rearrange-

ment or abnormalities [Popescu and Zimonjic, 2002; Zhang et al., 2007]. The potential for stem cells to become tumorigenic as the results of gene mutation is quite high since they are highly expanded in vitro [Kunkel and Bebenek, 2000; Han et al., 2005]. In this study the cytogenetic stability of oMSC and bMSCs was determined by comparing their karyotype at early and late passages. Our results showed that both oMSC and bMSCs were comparable showing a normal diploid karyotype and had an absence of aneuploidy or polyploidy. Normal chromosome structure was verified by G-banding analysis and abnormalities such as deletion, inversion, translocation, and rig chromosomes were not detected. These results suggest that there is only a limited possibility of oMSCs becoming tumorigenic as a result of extensive in vitro expansion.

Changes in proliferative gene expressions involve DNA replication, cell-cycle regulators, and chromatin modulators, all of which have been associated with replicative senescence [Wagner et al., 2008]. The *Wnt*, *bone morphogenetic protein*, and *Notch* pathways have been found to be implicated in key roles in self-renewal and differentiation of hematopoietic, intestinal, epidermal stem cells, and MSCs [Satija et al., 2007]. In this study we explored differences in expression of proliferative genes in MSCs sourced from patient-matched bone marrow and osteophytes tissues in relation to cell longevity. A total of 15 cell-cycle-related genes were investigated in oMSCs and bMSCs. It was found that 12 cell-cycle-related genes were similarly expressed between oMSCs and bMSCs, whereas the three genes *CCND2*, *APC*, and *BMP2* were differentially expressed, with a *P*-value <0.05. *CCND2* encodes proteins that amplify the G1 to S phase, thereby driving the cell cycle, although one study has shown that knockdown of *CCND2* only has a minor effect on cell division [Hishida et al., 2008]. Our study found that *CCND2* was approximately threefold down-regulated in oMSCs compared with bMSCs. This down-regulation of *CCND2* did not appear to affect the cell proliferation characteristics. *APC* plays a central role in *Wnt* signaling pathways which modulate stem cell survival [Kim et al., 2004] by negatively modulating the activity of cyclins [Bienz and

Hamada, 2004]. Down-regulation of *APC* expression in oMSCs may support their role in oMSC cell cycle. *BMP2* plays many regulatory roles in the maintenance of multipotency and "stemness" as well as differentiation of stem cells [Lecanda et al., 1997; Fromigue et al., 1998; Osyczka and Leboy, 2005], which may explain the observed unregulated *BMP2* expression in oMSCs.

In summary, osteophyte tissues contain pools of MSCs which exhibit normal traits, enter senescence after extended in vitro culture and have a normal karyotype compared to bMSCs. The greater longevity of oMSCs relative to bMSCs may be due to their origin from a regenerative tissue, in which the telomerase activity prevents telomere shortening in early cell culture, and thus delaying the point at which these cells succumb to replicative senescence.

ACKNOWLEDGMENTS

REFERENCES

Aida J, Izumiyama-Shimomura N, Nakamura K, Ishikawa N, Poon SS, Kammori M, Sawabe M, Arai T, Matsuura M, Fujiwara M, Kishimoto H, Takubo K. 2008. Basal cells have longest telomeres measured by tissue Q-FISH method in lingual epithelium. Exp Gerontol 43:833–839.

Baird DM. 2008. Mechanisms of telomeric instability. Cytogenet Genome Res 122:308–314.

Banfi A, Muraglia A, Dozin B, Mastrogiacomo M, Cancedda R, Quarto R. 2000. Proliferation kinetics and differentiation potential of ex vivo expanded human bone marrow stromal cells: Implications for their use in cell therapy. Exp Hematol 28:707–715.

Banfi A, Bianchi G, Notaro R, Luzzatto L, Cancedda R, Quarto R. 2002. Replicative aging and gene expression in long-term cultures of human bone marrow stromal cells. Tissue Eng 8:901–910.

Bernardo ME, Zaffaroni N, Novara F, Cometa AM, Avanzini MA, Moretta A, Montagna D, Maccario R, Villa R, Daidone MG, Zuffardi O, Locatelli F. 2007. Human bone marrow derived mesenchymal stem cells do not undergo transformation after long-term in vitro culture and do not exhibit telomere maintenance mechanisms. Cancer Res 67:9142–9149.

Bienz M, Hamada F. 2004. Adenomatous polyposis coli proteins and cell adhesion. Curr Opin Cell Biol 16:528–535.

Blackburn EH. 2001. Switching and signaling at the telomere. Cell 106:661–673.

Britt-Compton B, Wyllie F, Rowson J, Capper R, Jones RE, Baird DM. 2009. Telomere dynamics during replicative senescence are not directly modulated by conditions of oxidative stress in IMR90 fibroblast cells. Biogerontology C [Epub ahead of print].

Broccoli D, Young JW, de Lange T. 1995. Telomerase activity in normal and malignant hematopoietic cells. Proc Natl Acad Sci USA 92:9082–9086.

Cawthon RM. 2002. Telomere measurement by quantitative PCR. Nucleic Acids Res 30:e47.

Colter DC, Class R, DiGirolamo CM, Prockop DJ. 2000. Rapid expansion of recycling stem cells in cultures of plastic-adherent cells from human bone marrow. Proc Natl Acad Sci USA 97:3213–3218.

Counter CM, Gupta J, Harley CB, Leber B, Bacchetti S. 1995. Telomerase activity in normal leukocytes and in hematologic malignancies. Blood 85:2315–2320.

Dhaene K, Van Marck E, Parwaresch R. 2000. Telomeres, telomerase and cancer: An up-date. Virchows Arch 437:1–16.

Dimri GP, Lee X, Basile G, Acosta M, Scott G, Roskelley C, Medrano EE, Linskens M, Rubelj I, Pereira-Smith O, Peacock M, Campisi J. 1995. A biomarker that identifies senescent human cells in culture and in aging skin in vivo. Proc Natl Acad Sci USA 92:9363–9367.

Fehrer C, Brunauer R, Laschober G, Unterluggauer H, Reitinger S, Kloss F, Gully C, Gassner R, Lepperdinger G. 2007. Reduced oxygen tension attenuates differentiation capacity of human mesenchymal stem cells and prolongs their lifespan. Aging Cell 6:745–757.

Flores I, Canela A, Vera E, Tejera A, Cotsarelis G, Blasco MA. 2008. The longest telomeres: A general signature of adult stem cell compartments. Genes Dev 22:654–667.

Fromigue O, Marie PJ, Lomri A. 1998. Bone morphogenetic protein-2 and transforming growth factor-beta2 interact to modulate human bone marrow stromal cell proliferation and differentiation. J Cell Biochem 68:411–426.

Fujiwara T. 2009. Telomerase-specific virotherapy for human squamous cell carcinoma. Expert Opin Biol Ther 9:321–329.

Han C, Zhang X, Xu W, Wang W, Qian H, Chen Y. 2005. Cloning of the nucleostemin gene and its function in transforming human embryonic bone marrow mesenchymal stem cells into F6 tumor cells. Int J Mol Med 16:205–213.

Hanna CW, Bretherick KL, Gair JL, Fluker MR, Stephenson MD, Robinson WP. 2009. Telomere length and reproductive aging. Hum Reprod 24:1206–1211.

Harle-Bachor C, Boukamp P. 1996. Telomerase activity in the regenerative basal layer of the epidermis inhuman skin and in immortal and carcinoma-derived skin keratinocytes. Proc Natl Acad Sci USA 93:6476–6481.

Hayflick L. 1985. The cell biology of aging. Clin Geriatr Med 1:15–27.

Hishida T, Naito K, Osada S, Nishizuka M, Imagawa M. 2008. Crucial roles of D-type cyclins in the early stage of adipocyte differentiation. Biochem Biophys Res Commun 370:289–294.

Hiyama K, Hirai Y, Kyoizumi S, Akiyama M, Hiyama E, Piatyszek MA, Shay JW, Ishioka S, Yamakido M. 1995. Activation of telomerase in human lymphocytes and hematopoietic progenitor cells. J Immunol 155:3711–3715.

Kern S, Eichler H, Stoeve J, Kluter H, Bieback K. 2006. Comparative analysis of mesenchymal stem cells from bone marrow, umbilical cord blood, or adipose tissue. Stem Cells 24:1294–1301.

Kim KM, Calabrese P, Tavare S, Shibata D. 2004. Enhanced stem cell survival in familial adenomatous polyposis. Am J Pathol 164:1369–1377.

Kunkel TA, Bebenek K. 2000. DNA replication fidelity. Annu Rev Biochem 69:497–529.

Lecanda F, Avioli LV, Cheng SL. 1997. Regulation of bone matrix protein expression and induction of differentiation of human osteoblasts and human bone marrow stromal cells by bone morphogenetic protein-2. J Cell Biochem 67:386–396.

Mareddy S, Crawford R, Brooke G, Xiao Y. 2007. Clonal isolation and characterization of bone marrow stromal cells from patients with osteoarthritis. Tissue Eng 13:819–829.

Osyczka AM, Leboy PS. 2005. Bone morphogenetic protein regulation of early osteoblast genes in human marrow stromal cells is mediated by extracellular signal-regulated kinase and phosphatidylinositol 3-kinase signaling. Endocrinology 146:3428–3437.

Parsch D, Fellenberg J, Brummendorf TH, Eschlbeck AM, Richter W. 2004. Telomere length and telomerase activity during expansion and differentiation of human mesenchymal stem cells and chondrocytes. J Mol Med 82:49–55.

Popescu NC, Zimonjic DB. 2002. Chromosome and gene alterations in breast cancer as markers for diagnosis and prognosis as well as pathogenetic targets for therapy. Am J Med Genet 115:142–149.

Proctor A, Brownhill SC, Burchill SA. 2009. The promise of telomere length, telomerase activity and its regulation in the translocation-dependent cancer ESFT; clinical challenges and utility. Biochim Biophys Acta 1792:260–274.

Rubin H. 2002. The disparity between human cell senescence in vitro and lifelong replication in vivo. Nat Biotechnol 20:675–681.

Satija NK, Gurudutta GU, Sharma S, Afrin F, Gupta P, Verma YK, Singh VK, Tripathi RP. 2007. Mesenchymal stem cells: Molecular targets for tissue engineering. Stem Cells Dev 16:7–23.

Schmelzer E, Reid LM. 2009. Human telomerase activity, telomerase and telomeric template expression in hepatic stem cells and in livers from fetal and postnatal donors. Eur J Gastroenterol Hepatol [Epub ahead of print].

Serakinci N, Graakjaer J, Kolvraa S. 2008. Telomere stability and telomerase in mesenchymal stem cells. Biochimie 90:33–40.

Shaker OG, Hammam O, Salehd A, El Leithy T, Wishahi M. 2009. Possible role of telomerase and sFas in pathogenesis of various bladder lesions associated with schistosomiasis. Clin Biochem 42:864–872.

Simmons PJ, Torok-Storb B. 1991. Identification of stromal cell precursors in human bone marrow by a novel monoclonal antibody, STRO-1. Blood 78: 55–62.

Singh S, Jones BJ, Crawford R, Xiao Y. 2008. Characterization of a mesenchymal-like stem cell population from osteophyte tissue. Stem Cells Dev 17: 245–254.

van der Kraan PM, van den Berg WB. 2007. Osteophytes: Relevance and biology. Osteoarthritis Cartilage 15:237–244.

Wagner W, Horn P, Castoldi M, Diehlmann A, Bork S, Saffrich R, Benes V, Blake J, Pfister S, Eckstein V, Ho AD. 2008. Replicative senescence of mesenchymal stem cells: A continuous and organized process. PLoS ONE 3:e2213.

Wu YH, Cheng ML, Ho HY, Chiu DT, Wang TC. 2009. Telomerase prevents accelerated senescence in glucose-6-phosphate dehydrogenase (G6PD)-deficient human fibroblasts. J Biomed Sci 16:18.

Yang Q. 2008. Cellular senescence, telomere recombination and maintenance. Cytogenet Genome Res 122:211–218.

Yudoh K, Nishioka K. 2004. Telomerized presenescent osteoblasts prevent bone mass loss in vivo. Gene Ther 11:909–915.

Zhang ZX, Guan LX, Zhang K, Wang S, Cao PC, Wang YH, Wang Z, Dai LJ. 2007. Cytogenetic analysis of human bone marrow-derived mesenchymal stem cells passaged in vitro. Cell Biol Int 31:645–648.

Zimmermann S, Voss M, Kaiser S, Kapp U, Waller CF, Martens UM. 2003. Lack of telomerase activity in human mesenchymal stem cells. Leukemia 17:1146–1149.